

Global Λ polarization in heavy-ion collisions from a transport model

Hui Li,^{1,*} Long-Gang Pang,^{2,†} Qun Wang,^{1,‡} and Xiao-Liang Xia^{1,§}

¹*Department of Modern Physics, University of Science and Technology of China, Hefei, Anhui 230026, China*

²*Frankfurt Institute for Advanced Studies, Ruth-Moufang-Strasse 1, 60438 Frankfurt am Main, Germany*

The polarizations of Λ and $\bar{\Lambda}$ hyperons are important quantities in extracting the fluid vorticity of the strongly coupled QGP and the magnitude of the magnetic field created in off-central heavy-ion collisions, through the spin-vorticity and spin-magnetic coupling. We computed the energy dependence of the global Λ polarization in off-central Au+Au collisions in the energy range $\sqrt{s_{\text{NN}}} = 7.7 - 200$ GeV using A Multi-Phase Transport (AMPT) model. The observed polarizations with two different impact parameters agree quantitatively with recent STAR measurements. The energy dependence of the global Λ polarization is decomposed as energy dependence of the Λ distribution at freeze-out and the space-time distribution of the fluid-vorticity field. The visualization of both the Λ distribution and the fluid-vorticity field show a smaller tilt at higher beam energies, which indicates that the smaller global polarization at higher beam energies is caused by a smaller angular momentum deposition at mid-rapidity.

I. INTRODUCTION

In off-central heavy-ion collisions, huge orbital angular momenta of order $10^3 - 10^5 \hbar$ are generated. How such orbital angular momenta are distributed in the hot and dense matter is an interesting topic to be investigated. There is an inherent correlation between rotation and particle polarization. The Einstein-de-Haas effect [1] demonstrates that a sudden magnetization of the electron spins in a ferromagnetic material leads to a mechanical rotation due to angular momentum conservation. Barnett [2] proved the existence of the reverse process – the rotation of an uncharged body leads to the polarization of atoms and spontaneous magnetization. It is expected that quarks are also polarized in the rotating quark-gluon plasma (QGP) created in off-central heavy-ion collisions. Liang and Wang first proposed that Λ hyperons can be polarized along the orbital angular momentum of two colliding nucleus [3, 4]. Voloshin suggested that such a polarization can even be observed in unpolarized hadron-hadron collisions [5]. Besides the global orbital angular momentum, the local vorticity created by a fast jet going through the QGP also affects the hadron polarization [6]. The polarization density near equilibrium is first computed in the statistical-hydrodynamic model [7–9] and later confirmed in a quantum kinetic approach [10]. Some hydrodynamic calculations quantitatively predicted the global polarization in off-central heavy-ion collisions [11–14]. The fluid vorticity has also been investigated in transport simulations [15, 16]. For more studies of the fluid vorticity and Λ polarization, please refer to Refs. [17–24].

Recently STAR measured the global polarization of Λ and $\bar{\Lambda}$ in off-central Au+Au collisions in the Beam En-

ergy Scan (BES) program [25]. From the measured polarization, the fluid vorticity of the strongly coupled QGP and the magnitude of the magnetic field created in off-central heavy-ion collisions are extracted for the first time using the spin-vorticity and spin-magnetic coupling. It indicates that the rotational fluid has the largest vorticity, of order of 10^{21} s^{-1} , that ever existed in the universe. So the strongly coupled QGP has an additional extreme feature: it is the fluid with the highest vorticity. The global polarization of hyperons plays an important role in probing the vorticity field of the QGP. Therefore, it is worth to study the inherent correlation between the global polarization and the microscopic vortical structure in detail.

In this paper, we focus on the energy dependence of the vorticity field and global Λ polarization within A Multi-Phase Transport model (AMPT) [26] for nuclear-nuclear collisions in the energy range $\sqrt{s_{\text{NN}}} = 7.7 - 200$ GeV. The vorticity field profile given by AMPT is used to compute the global polarization of Λ and $\bar{\Lambda}$ produced in the hadron cascade using the spin-vorticity coupling. The paper is organized as follows: In Section II, we give the formula for the polarization induced by vorticity. In Section III, we introduce the numerical method we use. The numerical results and discussions are presented in Section IV. We finally give a summary in Section V.

In this paper we use the following conventions. The metric tensor is chosen as $g_{\mu\nu} = \text{diag}(1, -1, -1, -1)$ and the Levi-Civita symbol satisfies $\epsilon^{0123} = 1$. The symbols in boldface represent the spatial components of four-vectors, for example, $S^\mu = (S^0, \mathbf{S})$ denotes the spin four-vector and $u^\mu = \gamma(1, \mathbf{v})$ denotes the fluid velocity four-vector with $\gamma = 1/\sqrt{1 - \mathbf{v}^2}$ being the Lorentz factor.

II. Λ POLARIZATION FROM VORTICITY

In local thermal equilibrium, the ensemble average of the spin vector for spin-1/2 fermions with four-momentum p at space-time point x is obtained from

* lihui12@mail.ustc.edu.cn

† pang@fias.uni-frankfurt.de

‡ qunwang@ustc.edu.cn

§ xiaxl@mail.ustc.edu.cn

the statistical-hydrodynamical model [9] as well as the Wigner function approach [10] and reads

$$S^\mu(x, p) = -\frac{1}{8m} (1 - n_F) \epsilon^{\mu\nu\rho\sigma} p_\nu \varpi_{\rho\sigma}(x), \quad (1)$$

where the thermal vorticity tensor is given by

$$\varpi_{\mu\nu} = \frac{1}{2} (\partial_\nu \beta_\mu - \partial_\mu \beta_\nu), \quad (2)$$

with $\beta^\mu = u^\mu/T$ being the inverse-temperature four-velocity. In Eq. (1), m is the mass of the particle and $n_F = 1/[1 + \exp(\beta \cdot p \mp \mu/T)]$ is the Fermi-Dirac distribution function for particles ($-$) and anti-particles ($+$).

Some approximations can be made in Eq. (1) to simplify the computation of the global Λ polarization. First, since the temperature at freeze-out is much lower than the mass of the Λ , the number density of Λ 's is very small so that we can make the approximation $1 - n_F \simeq 1$ as in Ref. [11]. With this approximation, Eq. (1) is the same for Λ and $\bar{\Lambda}$. Care has to be taken since a finite chemical potential in n_F or spin-magnetic coupling could induce a difference between Λ and $\bar{\Lambda}$. However, the difference between the polarizations of Λ and $\bar{\Lambda}$ measured in the STAR experiment is not distinguishable within errors [25, 27]. For simplicity, we also do not distinguish Λ and $\bar{\Lambda}$ in the present research.

Second, the thermal vorticity $\varpi_{\mu\nu}$ in Eq. (2) contains the derivatives of u^μ and T . As pointed out in Ref. [20], the derivative of u^μ dominates over that of T during the evolution of the fireball, so we neglect ∇T and obtain

$$\varpi_{\mu\nu} \simeq \frac{1}{T} \Omega_{\mu\nu}, \quad (3)$$

where $\Omega_{\mu\nu}$ is the vorticity tensor defined by

$$\Omega_{\mu\nu} = \frac{1}{2} (\partial_\nu u_\mu - \partial_\mu u_\nu), \quad (4)$$

and the temperature at freeze-out is set to be $T = 160$ MeV.

Finally, Eq. (1) is rewritten as

$$S^\mu(x, p) = -\frac{1}{8mT} \epsilon^{\mu\nu\rho\sigma} p_\nu \Omega_{\rho\sigma}(x). \quad (5)$$

By decomposing the vorticity tensor in Eq. (4) into the following components,

$$\begin{aligned} \Omega_T &= (\Omega_{0x}, \Omega_{0y}, \Omega_{0z}) = \frac{1}{2} [\nabla \gamma + \partial_t (\gamma \mathbf{v})], \\ \Omega_S &= (\Omega_{yz}, \Omega_{zx}, \Omega_{xy}) = \frac{1}{2} \nabla \times (\gamma \mathbf{v}), \end{aligned} \quad (6)$$

Eq. (5) can be rewritten as

$$\begin{aligned} S^0(x, p) &= \frac{1}{4mT} \mathbf{p} \cdot \Omega_S, \\ \mathbf{S}(x, p) &= \frac{1}{4mT} (E_p \Omega_S + \mathbf{p} \times \Omega_T), \end{aligned} \quad (7)$$

where E_p , \mathbf{p} , m are the Λ 's energy, momentum, and mass, respectively.

The spin vector in Eq. (7) is defined in the center of mass (CM) frame of Au+Au collisions. In the STAR experiment, the Λ polarization is measured in the local rest frame of the Λ by its decay proton's momentum. The spin vector of Λ in its rest frame is denoted as $S^{*\mu} = (0, \mathbf{S}^*)$ and is related to the same quantity in the CM frame by a Lorentz boost

$$\mathbf{S}^*(x, p) = \mathbf{S} - \frac{\mathbf{p} \cdot \mathbf{S}}{E_p(m + E_p)} \mathbf{p}. \quad (8)$$

By taking the average of \mathbf{S}^* over all Λ particles produced at the freeze-out stage of AMPT, we obtain the average spin vector

$$\langle \mathbf{S}^* \rangle = \frac{1}{N} \sum_{i=1}^N \mathbf{S}^*(x_i, p_i), \quad (9)$$

where N is the number of Λ s in all events and i labels one individual Λ . The global Λ polarization in the STAR experiment is the projection of $\langle \mathbf{S}^* \rangle$ onto the direction of global angular momentum in off-central collisions (normal to the reaction plane),

$$P = 2 \frac{\langle \mathbf{S}^* \rangle \cdot \mathbf{J}}{|\mathbf{J}|}, \quad (10)$$

where we have included a normalization factor (P is normalized to 1) and \mathbf{J} denotes the global orbital angular momentum of off-central collisions.

III. MODEL SETUP

The string-melting version of the AMPT model is employed as event generator. It contains four stages: the initial condition, a parton cascade, hadronization, and hadronic rescatterings. In this model, the reaction plane is fixed to be the x - z plane where x is the direction of impact parameter \mathbf{b} and z is the beam direction as shown in Fig. 1. In off-central collisions, one nucleus centered at $(x = b/2, y = 0)$ in the transverse plane moves along the z direction, while the other nucleus centered at $(x = -b/2, y = 0)$ moves along the $-z$ direction, with $b \equiv |\mathbf{b}|$. The total angular momentum \mathbf{J} of the system and the global Λ polarization $\langle \mathbf{S}^* \rangle$ thus point along the $-y$ direction. However, the y -component of the local vorticity Ω_S (Ω_{zx}) is not forced to be negative everywhere in the fireball. In fact the local vorticity is a measure of local rotation in the comoving frame of one cell. Both relativistic fluid dynamics and transport models exhibit rich local vorticity structures [15–20, 23, 24]. The global angular momentum is the integral of local vorticity over all regions.

The AMPT model tracks the positions and momenta of all particles at any given time. These particles need to be fluidized on space-time grids in order to calculate

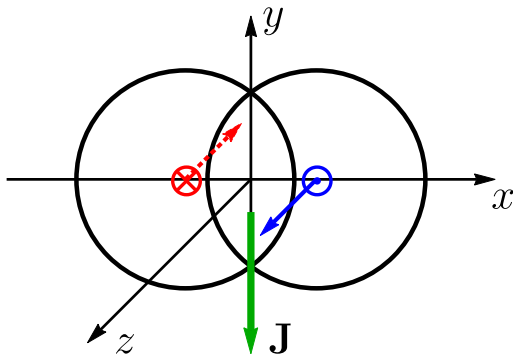


FIG. 1. Schematic picture of an off-central collision.

the velocity field numerically [15, 16, 28]. In the present study, the volume of the collision system is divided into 41×41 cells in the transverse plane with spacing $\Delta x = \Delta y = 0.5$ fm and 21 cells along the rapidity direction of size $\Delta\eta = 0.5$ unit. The velocity field in one cell is computed from the sum of energies and momenta of all particles in that cell, averaged over all events,

$$\mathbf{v}(t, x, y, z) = \frac{\sum_i \sum_j \mathbf{p}_{ij}}{\sum_i \sum_j E_{ij}}, \quad (11)$$

where \mathbf{p}_{ij} and E_{ij} denote the j -th particle's momentum and energy in a certain cell in the i -th event. For each BES energy and impact parameter (7 and 9 fm), we generate tens of thousands of events. In this way, the event-by-event fluctuation of the velocity is removed, so some event-by-event structures of the fluid, such as vortex pairings in the transverse plane due to hot spots [20] are wiped out. However, this is not a problem for the current study on the global Λ polarization since it is an integral effect of all regions and the local fluctuations are canceled or smeared when taking the sum over contributions. The obtained velocity field is used to calculate the relativistic vorticity for each cell following Eq. (4), using the finite-difference method (FDM). The spin vector of one Λ hyperon and the global polarization of all Λ hyperons are computed from the spin-vorticity coupling as given in Eqs. (7-10), using the values of the local vorticity in cells where Λ s freeze out kinetically (their final interaction point). For each chosen energy and impact parameter, we collect over 2 million Λ hyperons at the freeze-out stage.

IV. RESULTS AND DISCUSSIONS

A. Results for the Λ polarization

We run simulations at BES energies ranging from $\sqrt{s_{\text{NN}}} = 7.7$ GeV to 200 GeV. For each energy, we choose two fixed impact parameters $b = 7$ fm and 9 fm from the

range $b = 5.5 - 11.3$ fm corresponding to the 20% – 50% centrality class of the STAR experiment [29]. To match the Time Projection Chamber (TPC) region in the STAR experiment [25], the freeze-out Λ s are selected from the mid-rapidity region $|\eta| < 1$. We calculate the global Λ polarization from Eqs. (7-10) using the method described in Sec. III. The results are shown in Fig. 2.

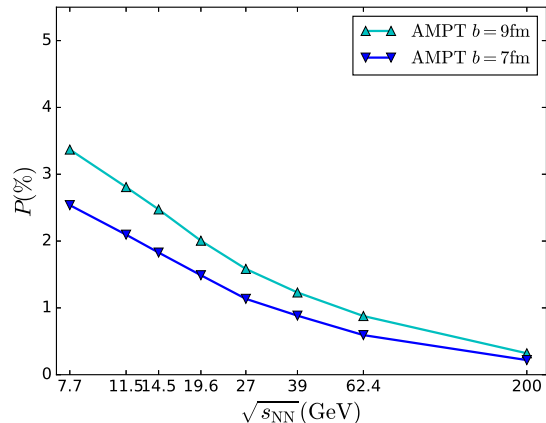


FIG. 2. The global Λ polarization at two impact parameters in Au+Au collisions.

As shown in Fig. 2, the global polarization is largest at $\sqrt{s_{\text{NN}}} = 7.7$ GeV and decreases as the beam energy increases. It almost vanishes at $\sqrt{s_{\text{NN}}} = 200$ GeV. The global polarization at $b = 9$ fm is larger than that at $b = 7$ fm at a specific energy. This is consistent with previous studies where the averaged and weighted vorticity increases with the impact parameter in the range $b < 10$ fm [15, 16]. The results shown in Fig. 2 only contain primary Λ hyperons that are directly produced at hadronization.

In practice, some Λ hyperons are secondary particles produced from resonance decays, like $\Sigma(1385) \rightarrow \Lambda + \pi$ (strong decay) or $\Sigma^0 \rightarrow \Lambda + \gamma$ (electromagnetic decay). It was shown in Ref. [30] that including feed-down Λ s decreases the global polarization. Different decay channels or decay parameters give different suppression factors. For direct decays and two-step cascade decays, the global polarization is estimated to be suppressed by about 17%, using the contributions to Λ from Ref. [29] and the decay branching ratios from Ref. [31]. For comparison, the suppression ratio is estimated to be 15% in Ref. [12] and 20% in Ref. [30].

In Fig. 3, the solid line represents the global polarization of primary Λ s from the average over two impact parameters. Primary plus feed-down Λ s result in a suppression of 17%, as shown by the dashed line, which is closer to the data than the one for primary Λ s only. The splitting between Λ and $\bar{\Lambda}$ is not included in the current study.

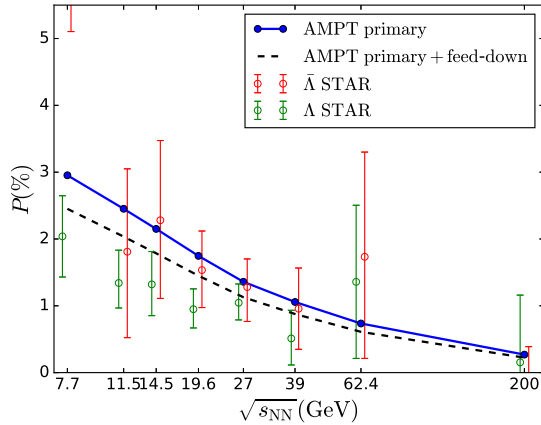


FIG. 3. The global Λ polarization at energies from 7.7 GeV to 200 GeV. Unfilled circles present the experimental measurements at STAR [25, 32].

B. Beam energy dependence of global polarization

The global polarization decreases as the collisional energy increases. This behavior contradicts the energy dependence of the global angular momentum. The reason for a small global polarization at high beam energy where angular momentum is large is investigated in this section. The global Λ polarization is given by the integral of a product of the Λ distribution $f_\Lambda(x)$ and the vorticity field $\Omega_{zx}(x)$,

$$P \sim \int d^4x f_\Lambda(x) \Omega_{zx}(x), \quad (12)$$

where x is the space-time point where Λ s kinetically freeze-out.

In the following, we investigate the energy dependence of f_Λ and Ω_{zx} and how they combine to determine the energy behavior of the polarization. We show $f_\Lambda(x)$ in Fig. 4 separately for $\sqrt{s_{NN}} = 7.7$ GeV and 200 GeV. The results at other BES energies between these two energies can be regarded as some kind of interpolation between them. We also select $b = 7$ fm for illustration.

Figure 4 shows the distribution of the Λ 's freeze-out position integrated over t and y , so it is a function of x and the space-time rapidity η . We see that f_Λ has a sideways tilt, namely more Λ are produced in the upper-right and lower-left region due to an asymmetric matter density distribution in off-central collisions. In the mid-rapidity region $|\eta| < 1$ (between the black dashed lines in Fig. 4) that we are interested in, f_Λ still shows a tilt at 7.7 GeV, but it is almost symmetric in both x and η at 200 GeV. The latter is the result of a broader range over which the fireball extends at higher energies so that the tilt can only be observed at large rapidity.

Figure 5 shows the relativistic vorticity Ω_{zx} in the reaction plane at $t = 5$ fm/c, which is a typical freeze-out

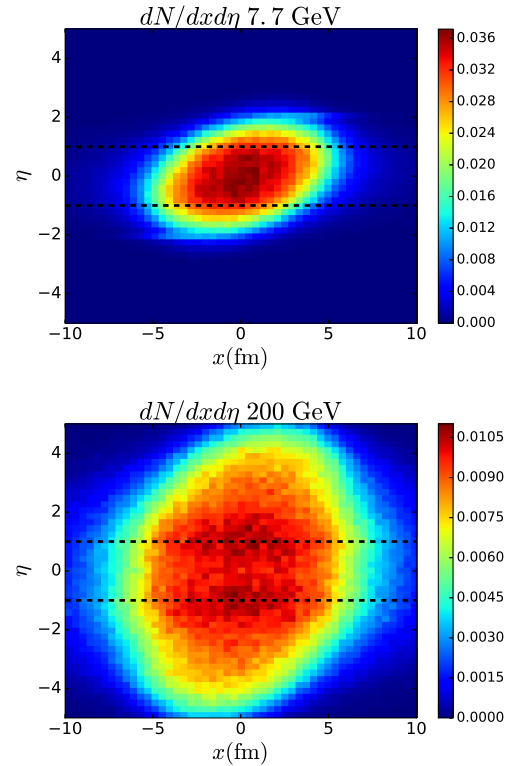


FIG. 4. The distribution of the Λ 's freeze-out positions integrated over t and y as a function of x and η (space-time rapidity). The mid-rapidity region $|\eta| < 1$ is between the black dashed lines.

time for Λ s in the mid-rapidity region. Here Ω_{zx} is not weighted by the particle number or energy density. We see that Ω_{zx} has the same magnitude at 7.7 and 200 GeV. However, our results show that the global Λ polarization at 7.7 GeV is about 10 times that at 200 GeV. Therefore the energy dependence of the global polarization cannot be explained by the magnitude of Ω_{zx} .

As displayed in Fig. 5, the vorticity field Ω_{zx} shows a quadrupole structure, i.e., it has opposite signs on different sides of each axis. Similar patterns are also found in other models or simulations [15, 19, 23, 24]. At 200 GeV the vorticity field Ω_{zx} is nearly a perfectly odd function of both x and η . This structure can be understood by the radial flow of the system, in which the transverse velocity v_x is an odd function of x but an even function of η [15]. However at 7.7 GeV the vorticity field Ω_{zx} is not an odd function as is evident by the fact that Ω_{zx} is non-vanishing in the central region $x \simeq 0$ or $\eta \simeq 0$.

Given the patterns of f_Λ and Ω_{zx} at 7.7 and 200 GeV, we now look at how they combine to give the global polarization. We know that Ω_{zx} is negative in the upper-right and lower-left region and leads to a Λ polarization along the $-y$ direction, and Ω_{zx} is positive in the upper-left and lower-right region and gives a Λ polarization along the $+y$ direction. When taking the average, these opposite polarizations cancel each other. Therefore the global

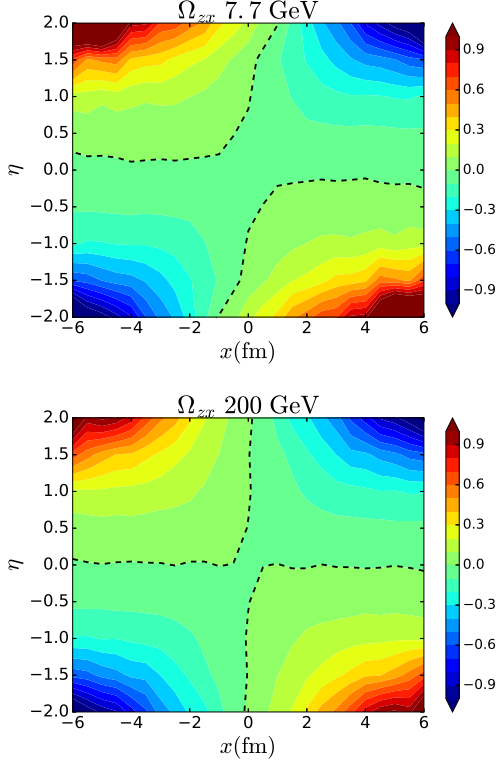


FIG. 5. The relativistic vorticity Ω_{zx} in units fm^{-1} on the reaction plane ($y = 0$) at $t = 5 \text{ fm}/c$ at $\sqrt{s_{\text{NN}}} = 7.7$ and 200 GeV. The black dashed lines represent the contour where $\Omega_{zx} = 0$.

polarization is determined by how many Λ hyperons are produced in the positive and negative-vorticity region.

At 200 GeV, Ω_{zx} (f_Λ) is nearly a perfectly odd (even) function in both x and η in the mid-rapidity region. There is almost an equal number of Λ hyperons produced in the positive and the negative vorticity region. Therefore the global Λ polarization is almost vanishing at 200 GeV. At 7.7 GeV, f_Λ is largest in the central region ($x, \eta \sim 0$) where Ω_{zx} is negative, which gives a global Λ polarization along the $-y$ direction.

The above argument is supported by Fig. 6 where we discretize the values of Ω_{zx} into several bins and count the number of Λ hyperons produced in the region with the specific Ω_{zx} value. More Λ hyperons are produced in the negative-vorticity region at 7.7 GeV, while an almost equal number of Λ hyperons is produced in both the positive and the negative-vorticity region at 200 GeV.

Both angular momentum and global polarization are related to the vorticity. The angular momentum is an integral effect of vorticity weighted by the moment of inertia over the volume of fireball,

$$\mathbf{J} = \int d^3x I(x) \boldsymbol{\omega}(x), \quad (13)$$

where $I(x)$ is the moment of inertia density of fireball and $\boldsymbol{\omega} = \nabla \times \mathbf{v}/2$ is the non-relativistic vorticity. The exact

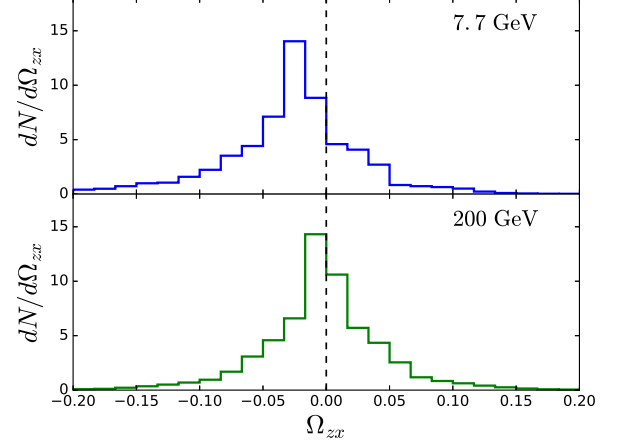


FIG. 6. The distribution of the number of Λ hyperons $dN/d\Omega_{zx}$.

form of $I(x)$ in fireball is not clear. A well motivated assumption is $I(x)$ being proportional to the particle number or energy density, see the discussions in [15]. The total amount of the moment of inertia increases with the collisional energy, and so does the total angular momentum of fireball. Such behavior is opposite to the global Λ polarization. However, in the mid-rapidity of fireball, the angular momentum decreases as the collisional energy increases, because $I(x)$ is nearly symmetric in the positive and the negative-vorticity region at high energy, just like $f_\Lambda(x)$. In this way, the energy dependence of Λ polarization can be understood by the smaller angular momentum deposited at mid-rapidity for higher beam energies. We also note that what happens in the mid-rapidity region at high energy is quite similar to the situation in central collision ($b = 0$), in which $f_\Lambda(x)$ and $I(x)$ (Ω_{zx} and ω_y) are exactly even (odd) functions of x and η , therefore even though non-zero vorticity is generated, the total angular momentum and global Λ polarization are vanishing after taking the integral (or average).

V. SUMMARY

In this paper we computed the global Λ polarization in Au+Au collisions at BES energies $\sqrt{s_{\text{NN}}} = 7.7 - 200$ GeV with the AMPT model. The observed global Λ polarization decreases as the beam energy increases. With feed-down Λ s from resonance decays, the computed polarization quantitatively agrees with experimental measurements at STAR.

To explain the energy dependence of the global Λ polarization, we computed the space-time distribution of the velocity field, vorticity field, and Λ s at freeze-out. The global polarization is obtained by summing over all space-time regions for the vorticity field weighted by the Λ 's distribution. We demonstrated that the deposited

angular momentum at mid-rapidity is smaller for higher beam energies, due to smaller sideways tilt and faster expansion.

ACKNOWLEDGEMENTS

The authors thank Yin Jiang, Jinfeng Liao, Zi-Wei Lin, Michael A. Lisa, Dirk H. Rischke, Zebo Tang, and

Zhangbu Xu for helpful discussions. HL, QW and XLX are supported in part by the Major State Basic Research Development Program (MSBRD) in China under the Grant No. 2015CB856902 and 2014CB845402 and by the National Natural Science Foundation of China (NSFC) under the Grant No. 11535012. LGP acknowledges funding through the Helmholtz Young Investigator Group VH-NG-822 from the Helmholtz Association and the GSI Helmholtzzentrum für Schwerionenforschung (GSI).

-
- [1] A. Einstein and W. J. de Haas, *Verh. Dtsch. Phys. Ges.* **17**, 152 (1915).
 - [2] S. J. Barnett, *Phys. Rev.* **6**, 239 (1915).
 - [3] Z. T. Liang and X. N. Wang, *Phys. Rev. Lett.* **94**, 102301 (2005) Erratum: [*Phys. Rev. Lett.* **96**, 039901 (2006)].
 - [4] J. H. Gao, S. W. Chen, W. t. Deng, Z. T. Liang, Q. Wang and X. N. Wang, *Phys. Rev. C* **77**, 044902 (2008).
 - [5] S. A. Voloshin, *nucl-th/0410089*.
 - [6] B. Betz, M. Gyulassy and G. Torrieri, *Phys. Rev. C* **76**, 044901 (2007).
 - [7] F. Becattini, F. Piccinini and J. Rizzo, *Phys. Rev. C* **77**, 024906 (2008).
 - [8] F. Becattini and F. Piccinini, *Annals Phys.* **323**, 2452 (2008).
 - [9] F. Becattini, V. Chandra, L. Del Zanna and E. Grossi, *Annals Phys.* **338**, 32 (2013).
 - [10] R. h. Fang, L. g. Pang, Q. Wang and X. n. Wang, *Phys. Rev. C* **94**, no. 2, 024904 (2016).
 - [11] F. Becattini, L. Csernai and D. J. Wang, *Phys. Rev. C* **88**, no. 3, 034905 (2013) Erratum: [*Phys. Rev. C* **93**, no. 6, 069901 (2016)].
 - [12] I. Karpenko and F. Becattini, *arXiv:1610.04717 [nucl-th]*.
 - [13] Y. L. Xie, M. Bleicher, H. Stöcker, D. J. Wang and L. P. Csernai, *Phys. Rev. C* **94**, no. 5, 054907 (2016).
 - [14] Y. Xie, D. Wang and L. P. Csernai, *Phys. Rev. C* **95**, no. 3, 031901 (2017).
 - [15] Y. Jiang, Z. W. Lin and J. Liao, *Phys. Rev. C* **94**, no. 4, 044910 (2016).
 - [16] W. T. Deng and X. G. Huang, *Phys. Rev. C* **93**, no. 6, 064907 (2016).
 - [17] L. P. Csernai, V. K. Magas and D. J. Wang, *Phys. Rev. C* **87**, no. 3, 034906 (2013).
 - [18] L. P. Csernai, D. J. Wang, M. Bleicher and H. Stöcker, *Phys. Rev. C* **90**, no. 2, 021904 (2014).
 - [19] F. Becattini *et al.*, *Eur. Phys. J. C* **75**, no. 9, 406 (2015).
 - [20] L. G. Pang, H. Petersen, Q. Wang and X. N. Wang, *Phys. Rev. Lett.* **117**, no. 19, 192301 (2016).
 - [21] A. Aristova, D. Frenklakh, A. Gorsky and D. Kharzeev, *JHEP* **1610**, 029 (2016).
 - [22] M. Baznat, K. Gudima, A. Sorin and O. Teryaev, *Phys. Rev. C* **88**, no. 6, 061901 (2013).
 - [23] O. Teryaev and R. Usubov, *Phys. Rev. C* **92**, no. 1, 014906 (2015).
 - [24] Y. B. Ivanov and A. A. Soldatov, *arXiv:1701.01319 [nucl-th]*.
 - [25] L. Adamczyk *et al.* [STAR Collaboration], *arXiv:1701.06657 [nucl-ex]*.
 - [26] Z. W. Lin, C. M. Ko, B. A. Li, B. Zhang and S. Pal, *Phys. Rev. C* **72**, 064901 (2005).
 - [27] I. Upsal for the STAR collaboration, talk given at Quark Matter 2017.
 - [28] D. Oliinychenko and H. Petersen, *Phys. Rev. C* **93**, no. 3, 034905 (2016).
 - [29] Z. Qiu, *arXiv:1308.2182 [nucl-th]*.
 - [30] F. Becattini, I. Karpenko, M. Lisa, I. Upsal and S. Voloshin, *arXiv:1610.02506 [nucl-th]*.
 - [31] K. A. Olive *et al.* [Particle Data Group], *Chin. Phys. C* **38**, 090001 (2014).
 - [32] B. I. Abelev *et al.* [STAR Collaboration], *Phys. Rev. C* **76**, 024915 (2007) Erratum: [*Phys. Rev. C* **95**, no. 3, 039906 (2017)].